Available online at www.sciencedirect.com
SCIENCE DIRECT
Polymer 46 (2005) 11548–11556
polymer
www.elsevier.com/locate/polymer

Pressure–volume–temperature dependencies of polystyrenes

L.A. Utracki *

National Research Council Canada, Industrial Materials Institute, 75 de Mortagne, Boucherville, Que., Canada J4B 6Y4

Received 9 August 2005; accepted 4 October 2005
Available online 24 October 2005

Abstract

The pressure–volume–temperature (*PVT*) dependencies of four molten polystyrenes (PS) were determined at $T=450$–530 K, and $P=0.1$–190 MPa. In addition, five sets of published *PVT* data for PS were examined. The Simha–Somcynsky (S–S) lattice-hole equation of state (eos) was used to analyze the data. Fitting the data to eos yielded the characteristic reducing parameters, viz. P^*, V^*, T^*, where from the Lennard–Jones measures of energetic (ε^*), and volumetric (v^*) interactions were calculated. It was found that: (1) the values of the interaction parameters for PS resins varied, viz. $27.7 \leq \varepsilon^* \leq 35.2$, and $35.5 \leq v^* \leq 50.2$; (2) ε^* was dependent on v^*, and (3) ε^* and v^* linearly increased with the logarithm of molecular weight. In addition, these volume-averaged interaction parameters depend on the chain configuration, as well as the presence of additives.

Keywords: Polystyrene; PVT behavior; Equation-of-state

1. Introduction

The pressure–volume–temperature (*PVT*) dependence of polymers has been measured to determine compressibility and the thermal expansion coefficients, important for process designing. However, these measurements, combined with adequate theoretical description, may provide an insight into the internal structure and the volume-averaged interactions. Several equations of state (eos) for liquids have been proposed [1–7]. In addition Tait empirical relation has been used [8]. Curro [9], Zoller [10], Rodgers [11], Rudolf et al. [12], reviewed and evaluated the suitability of several eos to describe the *PVT* behavior. Of the six mentioned theoretical expressions [11] the two: Dee and Walsh (D–W) modified cell model (MCM) [7], and Simha and Somcynsky (S–S) lattice-hole theory [4] performed well.

D–W modification of the Prigogine et al. cell model amounts to increasing the Lennard–Jones hard-core volume universally by 7%. The resulting eos provides good fit of data, with a set of characteristic reducing parameters (P^*, T^*, and V^*), and a single 'adjustable' quantity, M_0/c, where M_0 is segmental molecular weight, and $3c$ is the external degree of freedom [13].

The S–S theory has been used to provide description of the cohesive energy density [14,15], internal pressure, *PVT* behavior [16–20], etc. The great advantage of the S–S derivation is direct incorporation of the free volume parameter, h, which in turn may be used to interpret variety of dynamic properties, e.g. viscosity [21,22]. Considering the fundamental nature, precision, and wide applicability of the S–S theory, the following text will focus on the use of S–S eos. Fitting the experimental data to the eos yields the P^*, T^*, and V^* parameters, which are related to the Lennard–Jones 6–12 interaction quantities [23]: the maximum attractive energy, ε^*, and the segmental repulsion volume, v^*. For single-component polymeric liquids the *PVT* behavior is fully described by these two parameters through an adequate eos.

Over the years a large number of polymeric systems has been studied and the P^*, T^*, and V^* reducing parameters have been tabulated, e.g. see [9–12]. However, the P^*, T^*, V^* values published by various authors for supposedly the same polymer are different. Thus, this work aims to analyze the variability of the derived from S–S eos interaction parameters. Three potential sources will be examined: the method of testing (e.g. procedure, reproducibility), the computational methods, and variability of the tested material, viz. molecular weight and its distribution, additives introduced by the manufacturer, etc. Since the problem is general, for simplicity PS was selected. *PVT* data for several PS resins were measured in the author's laboratory, while additional sets were taken from literature.

* Tel.: +1 450 641 5182; fax: +1 450 641 5105.
E-mail address: leszek.utracki@cnrc-nrc.gc.ca

0032-3861/$ - see front matter © 2005 Elsevier Ltd. All rights reserved.
doi:10.1016/j.polymer.2005.10.020

2. Theory

The Simha–Somcynsky lattice-hole theory [4] considers an amorphous, condensed system as a mixture of occupied (by chain segments or small molecules) and empty sites. For macromolecules, the statistical segments are defined as $M_s = M_n/s$, where M_n is the number average molecular weight of a statistical macromolecule, composed of s statistical segments. The authors incorporated the configurational entropy of mixing as derived by Huggins and Flory for linear chains, and the inter-segmental interactions via the Lennard–Jones [23] (L–J) potential with the characteristic segmental energy, ε^*, and volume, v^*, per statistical segment:

$$E_0 = \lambda_{repuls} r^{-m} - \lambda_{attract} r^{-n}; \quad m = 10 \text{ to } 13; \quad n = 6 \text{ or } 7 \tag{1a}$$

The form of L–J potential (Eq. (1a)) was originally adopted because it provided satisfactory description for the second virial coefficient of a gas with m, $n > 4$. Later, the second attractive interactions term was derived using quantum mechanics (for hydrogen and helium, $n = 6$ and 7 was found, respectively). The first empirical term of Eq. (1a) has been identified as originating in repulsive interactions. Over the years the L–J potential (Eq. (1a) with $n = 6$, and $m = 12$) was applied to many condensed systems, quite different than these considered by L–J.

$$E_0 = \frac{qz\varepsilon^*}{s}\left[1.0109\left(\frac{v}{v^*}\right)^{-4} - 2.4090\left(\frac{v}{v^*}\right)^{-2}\right] \tag{1b}$$

Prigogine et al. [1,2] used the L–J mean-field relation to describe interactions between statistical segments of s-unit molecules (see Eq. (1b), in which the radius, r, of Eq. (1a) is replaced by cell volume, v). The authors also introduced the number $3c$ of the external, volume-dependent degrees of freedom, given by geometry and environment of each solvent molecule or polymeric segment. For linear, flexible molecules [13]:

$$3c = s + K \tag{2}$$

Simha derived [24] $K = 3$, and this value has been used with S–S eos applied to low molecular weight solvents. For other eos' K is empirical, changing from one eos to the next ($K = 0.86$ or 1.78) [13]. However, for high molecular weight polymers, where the number of statistical segments $s \gg 3$, the simplifying relation, $3c/s \approx 1$, is usually employed.

In the S–S theory the variables of state, and derived quantities are scaled. The three characteristic scaling parameters of pressure, temperature, and volume are defined as [4]:

$$\left.\begin{aligned} P^* &= \frac{zq\varepsilon^*}{(sv^*)} \\ T^* &= \frac{zq\varepsilon^*}{(Rc)} \\ V^* &= \frac{v^*}{M_s} \end{aligned}\right\} \left(\frac{P^*V^*}{T^*}\right) M_s = \frac{Rc}{s} \tag{3}$$

In the cell model, $zq = s(z-2)+2$ is the number of interchain contacts in a lattice of coordination number z, and R is gas constant. Using the reduced variables (indicated by tilde), SS expression for the configurational free energy is a function of specific volume, $\tilde{V}$, temperature, $\tilde{T}$, and the hole fraction: $h = h(\tilde{V}, \tilde{T})$:

$$\tilde{F} \equiv \frac{F}{F^*} = \tilde{F}[\tilde{V}, \tilde{T}, h(\tilde{V}, \tilde{T})] \tag{4}$$

Since the theory is general, describing a common $\tilde{P}\tilde{V}\tilde{T}$ surface, the reduced coordinates of the critical point are universal [25], thus: $\varepsilon^* \propto T_c$; $\varepsilon^*/v^* \propto P_c$; $v^* \propto V_c$. From Eq. (4), the eos is derived in form of coupled equations:

$$3c[(U - 1/3)/(1-U) - yQ^2(3AQ^2 - 2B)/6\tilde{T}] + (1-s) - \left(\frac{s}{y}\right)\ln[(1-y) = 0] \tag{5}$$

$$\tilde{P}\tilde{V}\tilde{T} = (1-U)^{-1} + 2yQ^2(AQ^2 - B)/\tilde{T} \tag{6}$$

with the occupied site fraction $y = 1-h$, and notation: $Q = 1/(y\tilde{V})$, $U = 2^{-1/6}yQ^{1/3}$. The coefficients $A = 1.011$, and $B = 1.2045$ account for non-nearest neighbors interactions in face-centered cubic lattice with the coordination number $z = 12$. The coupled equations describe the PVT surface, and associated with it free volume function, $h = h(\tilde{V}, \tilde{T})$.

The optimum value of the reducing parameters (P^*, T^*, and V^*) is determined by fitting the experimental PVT-surface in the molten state to Eqs. (5) and (6). Historically, two methods have been used, the sequential [26], and simultaneous. The sequential method obtains T^* and V^* from the ambient pressure V vs. T data, and then P^* is computed from the pressure dependencies. However, its values vary with the selected set of $V = V(P, T = \text{const})$; hence P^* has to be averaged over the range of P and T [27].

During the last two decades the simultaneous least-squares (lsq) fit of all data to S–S eos has been employed, Thus for example, Scientist™ from MicroMath has been used [14–20]. Rapid convergence is obtained in two-steps: (1) fitting data to the polynomial expression [16], $\tilde{V} = \tilde{V}(\tilde{P}, \tilde{T})$, provides the initial values of P^*, T^*, and V^*, and then (2) fitting the data to the coupled Eqs. (5) and (6). The computation provides numerical values of $h = h(\tilde{P}, \tilde{T})$, as well as the characteristic parameters: P^*, T^*, and V^*, from which the volume-averaged interaction parameters, ε^* and v^*, may be calculated using Eq. (3). It can be shown that h decreases as ε^* increases [20].

Table 1
Polystyrenes studied in this work

No.	Polymer code	Manufacturer	M_w (kg/mol)	M_n (kg/mol)	Ref.
1	PS-667	Dow Chem. Co.	215	?	This work
2	BASF 1424	BASF	261	–	This work
3	HH105	Monsanto	264	–	This work
4	PS 1301	Nova Chem.	270	–	[19]
5	Styron-686	Dow Chem. Co.	279	90.7	[11,29,30]
6	Z-110	Polyscience, Inc.	110	104	[28]
7	Z-34	Polyscience, Inc.	34.5	32.6	[28]
8	Z-9	Polyscience, Inc.	9.5	9.0	[28]
9	Z-09	Scientific polymer products	0.91	0.78	[28]

3. Experimental

Nine PS resins are listed in Table 1. Of these the first four were measured in this laboratory, using a Gnomix™ *PVT* apparatus (Gnomix Inc., Boulder, CO) [28], at $T=300$–530 K, and $P=0.1$–190 MPa. The molten state was observed at temperatures $T\cong 370$–530 K. The average error of these measurements was $\leq \pm 0.03\%$.

The initial work was carried out using injection molding grade PS-667 (MFR = 8 g/10 min; density $\rho=1040$ kg/m^3), containing 700 ppm Zn-stearate, and 2.5% mineral oil. Two types of measurements were conducted:

1. Isobaric, where at each selected P level the V is measured up to the highest T, then the material is cooled down, P is increased to the next level and $V=V(T)$ is measured, etc.

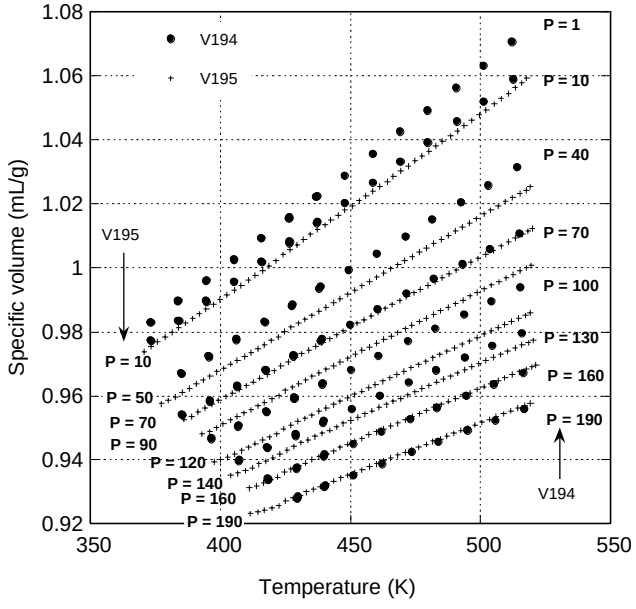

Fig. 1. Comparison between isothermal run #194 and isobaric run #195.

Table 2
Reducing parameters for PS Styron-686 as reported by different authors

No.	Method	P^* (bar)	T^* (K)	$10^4\times V^*$ (mL/g)	M_s	Ref.
1	Sequential	7453	12680	9598	49.12	[29]
2	Simultaneous	7155	12791	9627	51.42	[30]
3	Simultaneous	7159	12840	9634	51.61	[11]
4	Simultaneous, polynomial	7139±41	12811±49	9630±8	51.64	[16]
5	Simultaneous, exact	6995±75	12684±81	9623±13	52.22	[22]

Thus, the procedure requires n-heating cycles, where n is the number of selected P-levels.

2. Isothermal, where at each set temperature P is step-wise increased. Thus, the sample sees the highest temperature only once, at the end of the cycle.

The apparatus is supposed to take reading only when the P and T reached constant values. To test this, for some isothermal runs additional holding time was used ($t_h=30$ and 90 s). The tests were repeated until the difference of V between two consecutive runs was smaller than ± 0.0002 mL/g. Examples of raw data are presented in Fig. 1. The extracted characteristic parameters and statistics of fit are listed in Table 2.

Thus, the *PVT* measurements were found reproducible. For PS the isothermal and isobaric modes gave comparable results with the automatic holding time. However, as shown in Table 3, increasing the holding time (by 30 or 90 s) improved accuracy. Combining data from all runs considerably reduces the standard error of measurements, viz. for P^*, T^*, and V^* ± 0.15, ±0.08, and ±0.02%, respectively.

4. Calculations

4.1. Sequential vs. the simultaneous data fit

Quach and Simha [29] studied the *PVT* behavior of Styron 686 (Table 1) at $T=7.7$–195.6 °C, and $P=1$–2000 bar, measuring the specific volume, $V\pm 0.0002$ mL/g. The authors computed the characteristic parameters: P^*, T^*, and V^* using the sequential method, and assuming that $3c/s=1$. The obtained parameters are listed in Table 2.

The same experimental data were later recomputed using the simultaneously fit by Hartmann et al. [30], Rodgers [11], and Utracki and Simha [16,22]. Within the range of experimental error the simultaneous fits by different authors and/or different programs gave more consistent and reliable results, than those obtained using the sequential calculations. As a consequence, the sequential method should not be used.

4.2. Simultaneous data fit

The characteristic reducing parameters for the commercial PS were computed by simultaneously fitting the coupled Eqs. (5) and (6) to experimental data. For the commercial, high

Table 3
The characteristic reducing parameters and the statistical fit data for PS-667, and for the other commercial resins: BASF-1424, HH105, and PS-1301

Run #	Test type	P^* (bar)	T^* (K)	$10^4 \times V^*$ (mL/g)	M_s	σ	r^2
190	Isobar.	7769±16	11743±13	9534.8±2.7	43.998	0.000506	0.9999997
192	Isobar.	7743±17	11746±13	9526.4±2.7	44.081	0.000534	0.9999997
193	Isobar.	7718±16	11735±12	9529.1±2.6	44.243	0.000509	0.9999997
195	Isobar.	7767±19	11746±15	9503.1±3.2	44.105	0.000656	0.9999996
All isobaric		7740±10	11728±8	9502.1±1.7	44.193	0.000681	0.9999995
194	Isoth. 30	7385±31	11610±26	9505.3±5.5	45.839	0.000737	0.9999994
196	Isoth. 90	7442±26	11706±21	9525.3±4.6	45.769	0.000752	0.9999997
222	Isoth. aut	7662±44	11626±36	9520.8±8.0	44.168	0.000851	0.9999993
All isothermal		7742±13	11745±9	9530.8±2.0	44.40	0.000670	0.9999995
Average PS-667		7741±12	11736±9	9516±2	44.30	0.000681	0.9999995
BASF 1424		8134±15	11379±9	9477±2	40.976	0.000613	0.9999996
HH105		8111±16	11265±9	9339±2	41.210	0.000622	0.9999996
PS 1301		7435±26	11723±22	9526±5	45.869	0.001111	0.9999987

Note: runs #190, 192, 193, and 195 were isobaric, runs #194 and 196 were isothermal with the hold time $t_h = 30$ and 90 s, respectively, and #222 isothermal—automatic ($t_h = 0$ s).

molecular weight (MW) resins (MW > 200 kg/mol; hence $s >$ 3800) $3c/s = 1$ was assumed.

The computed values of P^*, T^*, and V^* are listed in Table 3, along with the statistics of fitting ($\sigma =$ standard deviation; $r^2 =$ correlation coefficient squared). The S–S eos well represents the observed dependencies.

4.3. Narrow MWD PS

The simultaneous fitting was also used for the *PVT* data reported for the low molecular weight PS [28], with narrow molecular weight distribution (MWD), $M_w/M_n = 1.06$–1.16 (polymers #6–9 in Table 1). The fitting of Eqs. (5) and (6) to the published data was carried allowing for the variability of the external degree of freedom ($3c = s + 3$). As shown in Table 4, computations resulted in good fit to data. It is noteworthy that even when $M_s \cong 52.07 = M_0/2$ was constant, the characteristic parameters systematically varied with MW.

Briefly, the results listed in Tables 2–4 indicate that:

1. The molar mass of statistical segment, $M_s \leq 52$; hence in commercial PS the number of statistical segments, $s \gg 3$, and the assumption that $3c/s \cong 1$ is valid.
2. For low MW PS $M_s \cong 52$ was computed assuming that $3c = s + 3$, i.e. the molar mass of PS statistical segment is about equal 1/2 styrene mer: $M_s \cong M_0/2$.
3. The characteristic parameters of PS resins vary widely, viz. $P^* = 6995 - 8134$ bar, $T^* = 10{,}001 - 12{,}840$ K, and $V^* = 0.9339 - 0.9832$ mL/g. Since their average experimental errors are, respectively, ±30 bar, ±31 K, and ± 0.0005 mL/g, the variability is well outside the range of experimental uncertainty.

5. Interaction parameters

Eq. (3) relates the three characteristic scaling parameters P^*, T^*, V^* to the intersegmental interactions. Since S–S eos is 'mean-field', the extracted parameters are volume-averages, expected to vary with molecular configuration and purity. From Eq. (3), taking the lattice of coordination number as $z = 12$:

$$\varepsilon* = \frac{T^* R c}{z q} \cong \left(\frac{T^* R}{3}\right)\left(\frac{3c}{[10s + 2]}\right) = \frac{v^* P^*}{(10 + 2/s)} \tag{7a}$$

$$v^* = V^* M_s$$

For low molecular weight solvent-type liquids (e.g. *n*-paraffins) the computer program optimizes the s and c parameters, thus Eq. (7a) may be used directly. For polymer melts, where $s \gg 3$ the Eq. (7a) may be simplified to read:

$$\varepsilon^* \cong 2.771 T^*; \quad v^* = V^* M_s \tag{7b}$$

6. Discussion

6.1. Correlation between ε* and v* in PS

The first dependence in Eq. (3) combines the two interaction parameters. For high molecular weight linear molecule melts ($s \gg 3$):

$$v^* = \left(\frac{zq}{s}\right)\left(\frac{\varepsilon^*}{P^*}\right); \quad \text{but if :} \quad \frac{zq}{s} = z - 2 + 2/s \to 10 \tag{8}$$

$$\underbrace{v^* \cong \frac{10\varepsilon^*}{P^*} \quad \text{or} \quad \varepsilon^* \cong \frac{v^* P^*}{10}}_{\text{for polymers}}$$

Table 4
Reducing parameters for PS with low MW, computed assuming $3c = s + 3$

PS	P^* (bar)	T^* (K)	$10^4 \times V^*$ (mL/g)	$3c/s$	M_s	σ	r^2
Z-110	7373±71	11475±70	9615±9	1.161	52.081	0.00085	0.9999993
Z-34	7821±31	11187±42	9631±6	1.265	52.066	0.00056	0.9999997
Z-9	7902±30	10989±38	9667±6	1.306	52.067	0.00056	0.9999997
Z-09	7759±28	10050±25	9839±4	1.427	52.062	0.00101	0.9999990

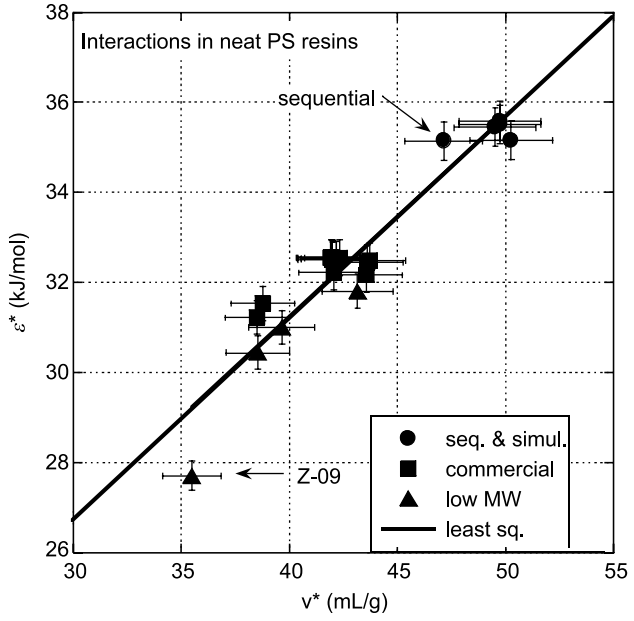

Fig. 2. The relation between the interaction parameters ε^* vs. v^* for PS resins listed in Tables 2–4. The line represents Eq. (9).

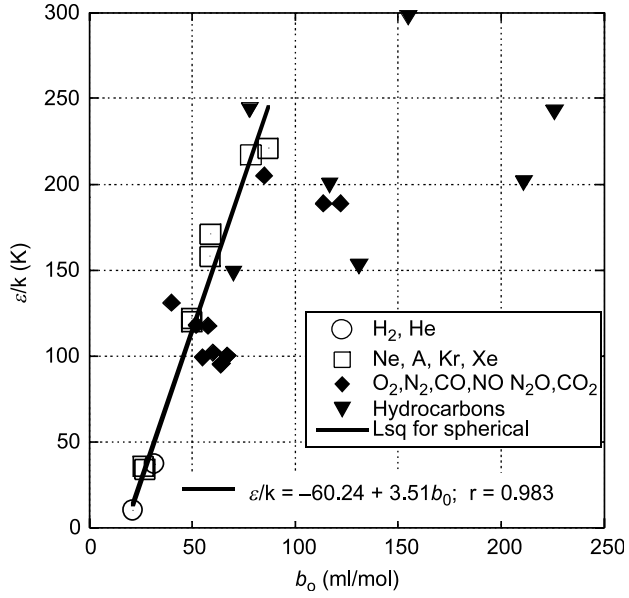

Fig. 3. The relation between the L–J force constants, ε vs. v_0, for light and noble gases, as well as for simple polyatomic molecules.

Thus, when P^* is approximately constant these parameters should be proportional to each other. The P^* in Tables 2–4 varies within $\pm 4.8\%$, i.e. a correlation between ε^* and v^* is expected.

Fig. 2 displays an inter-relation between ε^* and v^* for all examined PS resins:

$$\varepsilon^* = a_0 + a_1 v^* \tag{9}$$

$$a_0 = 13.44; \quad a_1 = 0.445; \quad r = 0.952$$

This lsq dependence was computed for all data points including the two deviating ones: a result of sequential fitting S–S eos to PVT data of Styron 686, and computed for the lowest molecular weight PS Z-09. The experimental error of measurements is indicated. According to Fig. 2 the L–J interaction parameters for supposedly the same chemical species are not constant. The values for the three low molecular weight PS's from Polyscience are important for understanding the behavior. In spite of their low polydispersity they follow the same dependence as the polydispersed commercial resins with additives. Furthermore, their interaction parameters increase with MW (Table 4). An exception is the lowest MW sample with $M_n = 780$ g/mol—a mixture of penta- and hexa-mers. Its energetic interaction parameter is smaller, or v^* larger, than expected from the empirical dependence given by Eq. (9).

Mathematically, the parameters, ε^* and v^*, define the minimum of the L–J potential, Eq. (1), with ε^* being the maximum attractive energy at the potential minimum, i.e. for $r = 2^{1/6} v^{*1/3}$. Thus, the empirical Eq. (9) means that as the strength of interaction increases the minimum of the L–J potential occurs at the increasing distance between centers of the interacting segments. The phenomenon seems to be general—the plot of the L–J force constants for gases [31] is displayed in Fig. 3 (note: the symbols and units are left the same as in [25]).

The linear dependence with high correlation coefficient was obtained for light and noble gases having roughly spherical interacting atoms or molecules. The two-atom gases (e.g. N_2, O_2, CO, NO) approximately follow the dependence, but the three-atom ones (CO_2 or N_2O) and hydrocarbons, C_nH_{2n+2} (for $n \geq 3$) progressively deviate from it. Thus, for non-polar, low density gases the correlation between ε and v_0 depends on the size and/or geometry of the interacting species. The linear dependence of ε^* on v^* was also observed for liquid *n*-paraffins measured within the AIP research project [32]. In short, the linear relation between the L–J characteristic interaction parameters is general, observed for gasses, low molecular weight liquids, and molten polymers.

In spite of similar dependencies shown in Figs. 2 and 3, the interaction mechanisms in low-density gases and condensed systems are quite different [1,23,25]. In the S–S lattice-hole theory the size of cell is unspecified, but 'self-adjusting'. However, since the computed segmental mass of statistical segment, M_s, is nearly constant, the cells that accommodate PS segments should have similar size. Nevertheless, the characteristic interaction parameters depend on the type and grade of PS resin. The narrow MW PS [28] samples have well defined MW and MWD; Fig. 2 suggests a relation between the interaction parameters and MW.

6.2. Molecular weight dependence of ε^* and v^* for PS

6.2.1. Ougizawa et al. approach

Ougizawa et al. [13] investigated the MW dependence of the characteristic scaling parameters P^*, T^*, V^*, calculated for 11 narrow MWD oligo- and poly-styrenes. The authors used Flory

Table 5
Reducing parameters of MCM eos for PS with low MWD

PS	P^* (bar)	T^* (K)	$10^4 \times V^*$ (ml/g)	M_0/c	σ	r^2
Z-110	5620±60	6413±23	8680±8	109.29	0.00091	0.9999992
Z-34	5837±24	6375±15	8704±5	104.32	0.00058	0.9999996
Z-9	5888±25	6308±15	8741±5	101.89	0.00062	0.9999996
Z-09	5746±24	5848±10	8906±4	95.00	0.00112	0.9999988

et al. [3] and D–W [7] eos' to fit the *PVT* data. Zoller and Walsh published [28] *PVT* measurements for four of these samples (Table 4). To interpret the observed MW dependence of P^*, T^*, V^*, Ougizawa et al. postulated that macromolecules have two types of interacting segments: end-groups, and the others. Thus, the characteristic scaling and other parameters were expected to follow a hyperbolic dependence:

$$X = X_\infty + \frac{K}{M}; \quad X \in \left(P^*, T^*, V^*, \frac{c}{M_0}, T_g\right) \tag{10}$$

where K= constant, and X_∞ is the parameter value for $M \gg K$. The plots of X vs. $1/M$ indicated that only low molecular weight resins ($M < 10$ kg/mol) follow Eq. (10).

To examine validity of Eq. (10) the *PVT* data [28] for the four samples were fitted to D–W MCM eos [7]. The extracted parameters, and statistics of fit, are listed in Table 5, where the values of parameter $M_0/c = RT^*/P^*V^*$ are also given. The MW dependencies of c/M_0 and V^* are presented in Fig. 4—evidently Eq. (10) is not valid. A similar relation was obtained for T^*. However, since parameter P^* is a function of the ε^*/v^* ratio, a simple MW dependence was neither expected nor found.

Evidently, Eq. (10) should be valid for MW dependence of the glass transition temperature (T_g). Using the free volume argument, Fox and Flory [33] derived such a dependence, and for PS they showed that: $T_g(°C) = 100–1800/M_n$ (kg/mol). The relation was later reported valid for 'sufficiently high' MW [34]. However, it is not justifiable to expect that the MW dependence valid for T_g would be followed by the inter-segmental interactions in the molten state [35].

6.2.2. Interaction parameters obtained from S–S eos

Fig. 4 shows that Eq. (10) is not valid for the *PVT* characteristic scaling parameters. Instead, the data for c_0/M, V^* and T^* well correlate with log M_w, i.e.:

$$\frac{\partial X}{\partial M_w} \propto \frac{1}{M_w} \Rightarrow X = X_0 + X_1 \log M_w \tag{11}$$

Thus, it seems that, at least for PS, the end-groups do not play any special role.

The binary interaction parameters, ε^* and v^*, were calculated from P^*, T^*, and V^* (Tables 2–4) using Eq. (7a). The M_w values for the four low MWD are available [28]. The manufacturers provided M_w values for the commercial resins: PS-667, PS-1301, and Styron 686. Those for BASF 1424 and HH105 were calculated from the dynamic rheology at three temperatures.

Fig. 5 shows that in agreement with Eq. (11), the interaction parameters increase with logarithm of M_w. The lines in Fig. 5

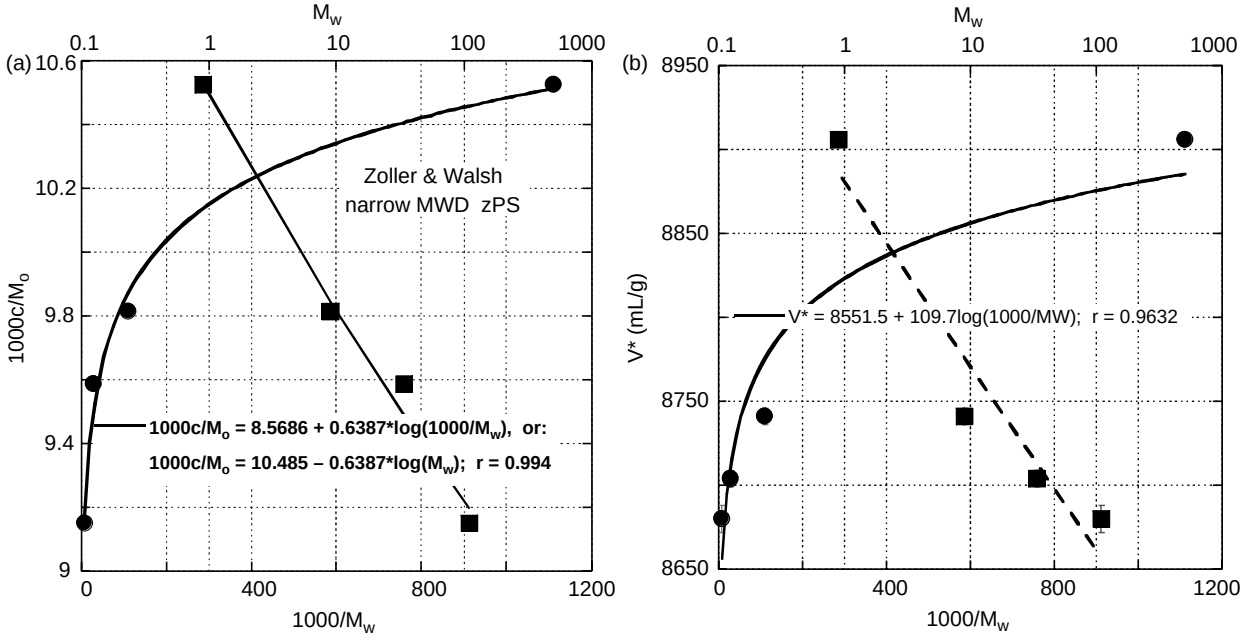

Fig. 4. (a) c/M_0 values are plotted vs. $1/M_w$ (circles) or vs. log(M_w) (squares). The lines represent logarithmic dependence shown in the figure. (b). V^* values are plotted vs. $1/M_w$ (circles) or vs. log(M_w) (squares). The lines represent logarithmic dependence shown in the figure.

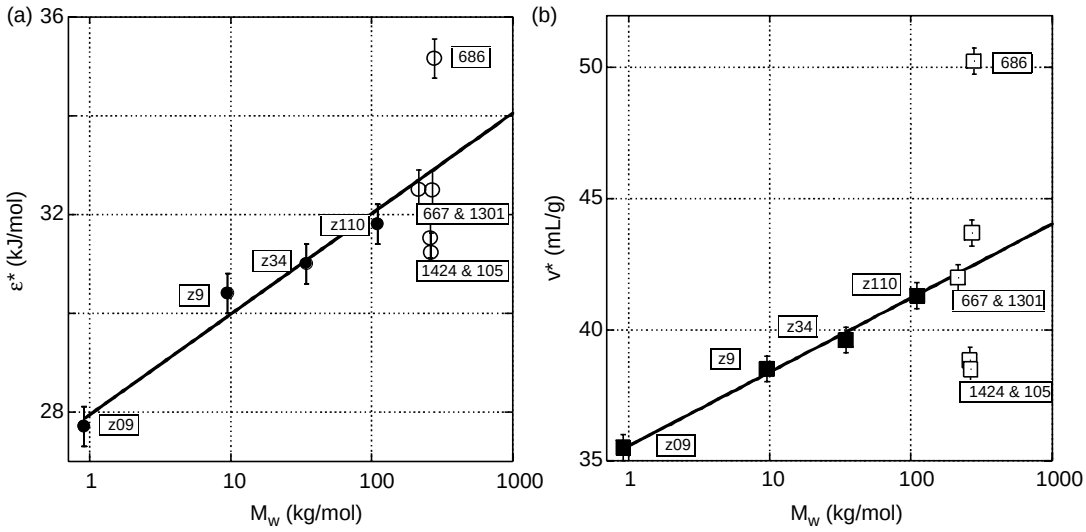

Fig. 5. Molecular weight dependence for ε^* (left) and v^* (right) of low molecular weight distribution PS samples [28], and commercial PS resins. Error bars for the interaction parameters are shown. The lsq lines are given by Eq. (12). The samples are identified by numbers from Table 1.

are the lsq empirical dependencies calculated for the narrow MWD samples [28]:

$$\varepsilon^* = 27.95 + 2.03\log(M_w); \quad r = 0.992 \tag{12}$$

$$v^* = 35.57 + 2.83\log(M_w); \quad r = 0.998$$

These relations are also valid for PS-667 and PS-1301, but the other three commercial resins (BASF 1424, HH105, and Styron 686) deviate from them. However, the deviation for both interaction parameters is in the same direction, thus the plot of ε^* vs. v^* in Fig. 2 is common for all tested samples, independently of the departure from the common MW dependence.

For the commercial high MW PS resins the values of the interaction parameters ranges: $\varepsilon^* = 31.2$–35.2, and $v^* = 38.5$–50.2. Evidently, the spread far exceeds the experimental error of the *PVT* measurements. Thus, in addition to MW effects, the interaction parameters for these resins depend on PS-chain configuration, as well as on the amount of impurities from polymerization, additives, and modifiers.

According to the theoretical Eq. (2), the MW dependence of the segmental degree of freedom $3c/s$ should follow Eq. (10). However, the values extracted from the *PVT* dependencies contradict this expectation; instead Eq. (11) provides good approximation, viz.:

$$\frac{3c}{s} = 1.47 - 0.184\log M_w; \quad r = 0.961 \tag{13}$$

6.2.3. Interaction parameters in other systems

Application of the S–S eos to *PVT* of several PS resins shows that the extracted interaction parameters, ε^* and v^*, are inter-related, and that their values depend on MW. These observations seem to be applicable to other polymers, solvents, and polymeric nanocomposites. Linear relationships between ε^* and v^* were obtained for several polymeric [11], and non-polymeric (data from reports of API Project 42 [32]) systems. For paraffins, the data were simultaneously fitted assuming that all five parameters are adjustable: c, s, P^*, T^*, and V^*. The S–S eos fitted the data well, viz. the standard deviation $\sigma = 0.00041$ and $r^2 = 0.9999999$. The values of Eq. (9) parameters and correlation coefficient, r, are listed in Table 6.

6.2.4. Effect of the P*, T*, V* parameters on the PVT dependence

For the commercial resins listed in Table 1, the largest difference of ε^* vs. v^* parameters in Fig. 5 is between those of Styron 686 and HH105. Indeed, their reducing parameters P^*, V^*, T^* (listed in Tables 2 and 3, respectively) show the largest difference. Thus, it is desirable to examine the effect of these two sets of characteristic parameters on the *PVT* surface.

Fig. 6 displays the simulated *PVT* behavior of these two resins at the lowest and highest experimental pressure, $P = 1.0132$ and 2000 bar. The two resins have similar specific volumes, but their compressibility (κ) and thermal expansion (α) coefficients are significantly different. Styron-686 with

Table 6
Parameters of Eq. (9), and correlation coefficient

No.	Liquid	a_0	a_1	r	Range of v^*	Ref.
1	PS	13.44	0.445	0.952	35–50	This work
2	Dendrimers[a]	10.1	0.852	0.936	23–30	[36]
3	Fluoropolymers[b]	10.1	0.548	0.965	33–37	[37]
4	PP+C15A[c]	22.4	0.129	0.985	50–61	[20]
5	Polyolefins[d]	20.8	0.183	0.865	30–61	[11]
6	HT polymers[e]	21.1	0.399	0.904	25–40	[11]
7	*n*-paraffins	13.47	0.378	0.880	35–40	[32]

[a] Poly(benzyl ether) dendrimers MW = 1592–13,464 g/mol.
[b] Polyvinylidene fluorides and their copolymers with hexa-fluoro propylene.
[c] Polypropylene with 0–4 wt% of Cloisite® 15A.
[d] Polyethylene's and polypropylenes.
[e] Here the high temperature (HT) polymers are: polyethylene terephthalate, polyphenylene ether, polyarylates, polycarbonates, polyether-ether-ketone, polysulfones.

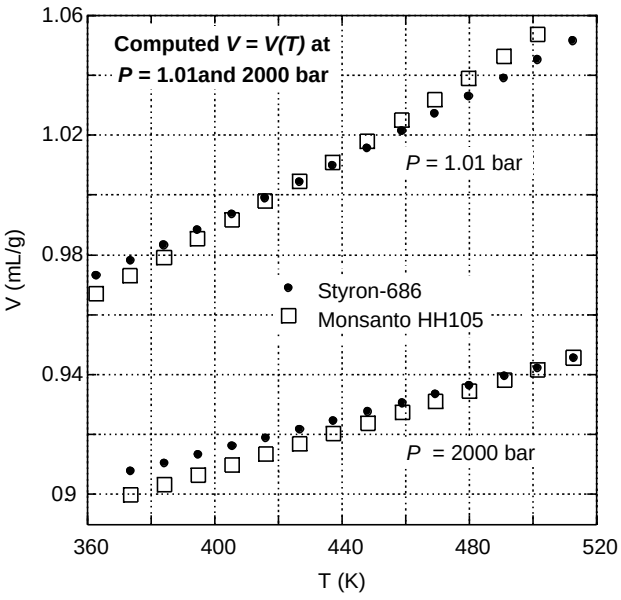

Fig. 6. Computed specific volume vs. temperature dependence at ambient pressure and at 2000 bar for PS resins: PS-686, and PS-HH105, listed in Tables 2 and 3, respectively.

higher value of the interaction parameters and lower free volume shows lower κ and α.

6.2.5. Fundamental consequences

Two correlations were discussed: (1) between the interaction parameters, ε^* vs. v^*, and (2) between the interaction parameter and M_w. The former relation might have been expected from the basic theorem of corresponding states [1], which requires for ε^* to be proportional to v^* when P^* is nearly constant.

However, the second correlation is more difficult to explain, as it implies that the segmental interactions are affected by the size of the whole molecule, while at the same time the statistical segment size (as measured by M_s) remains constant. By contrast with the transport properties, here the relation is the same below and above the entanglement molecular weight. The postulate that the dependence originates from different contribution of the macromolecular end and center groups was found invalid—instead good correlation was found between the interaction parameters and logarithm of MW.

Hirschfelder et al. [31] have shown that for gases v^* and ε^* are proportional to the critical volume and temperature, respectively. Considering that the corresponding states principle is to be valid also for condensed systems, this observation is expected to be general. Notably, the critical point parameters are known to depend on molecular parameters [38,39], viz. the critical volume and temperature show a different dependence on parachor; hence on the molar volume. This offer a support for the dependence presented in Fig. 3, and indirectly for the PS melts. Increase of the binary interaction parameters with molecular weight seems to be a general phenomenon. However, it is not obvious why these parameters should increase with logarithm of molecular weight for a series of PS samples, when the 'self adjusting' lattice cell size remains constant!

7. Summary and conclusions

The *PVT* behavior of nine polystyrenes was measured and analyzed using the Simha–Somcynsky equation of state (eos). The results may be summarized as follows:

1. Isobaric and isothermal methods of data acquisition result in similar sets of the characteristic reducing parameters, P^*, V^*, and T^*. The slightly larger scatter in isothermal than in isobaric runs, may be reduced by using longer holding time, e.g. 30 – 90 s. The specific volume in two consecutive runs was reproducible within ± 0.0002 mL/g.
2. Two principal methods of data fitting to eos are: (1) two-step requiring determination of V^*, and T^* from data at ambient pressure, followed by that of P^* from an isothermal run; and (2) simultaneous optimization of fit for all characteristic reducing parameters. The latter method is more reliable and should be used.
3. The S – S eos well describes the *PVT* behavior. For the examined PS resins the molar mass of a statistical segment, $M_s \cong M_0/2$, is about 1/2 of the molar mass of styrene.
4. The characteristic reducing parameters, P^*, V^*, and T^*, of the nine PS's showed significant variation of values, reflected in variation of the binary interaction parameters: the energetic, ε^*, and the volumetric, v^*.
5. Plot of ε^* vs. v^* was found to be linear for all PS resins. Similar linearity was observed for other molten polymers, polymeric nanocomposites, as well as for liquid paraffins. The correlation originates in the definition of the characteristic parameters, P^*, V^*, and T^*.
6. The ε^* and v^* parameters increase with the logarithm of molecular weight. Since these are mean-averaged quantities, their magnitude is also affected by polydispersity, chain configuration, impurities, additives, etc.
7. Simulation of the *PVT* behavior for two PS resins that showed the largest difference between the characteristic reducing parameters, P^*, V^*, and T^*, showed a similar *PVT* surface, but the derivative properties (e.g. the thermal expansion or compressibility) were quite different.
8. P^*, V^*, and T^*, depend on MW, chain configuration, reaction by-products, and additives. Furthermore, there are several sources of random and systematic errors (viz. experimental, computational, compositional) in determining them. Thus, for a given type of polymer there are many *PVT* dependencies.

References

[1] (a) Prigogine I, Trappeniers N, Mathot V. Discuss Faraday Soc 1953;15:93.
(b) Prigogine I, Trappeniers N, Mathot V. J Chem Phys 1953;21:559.
[2] Prigogine I, Bellemans A, Mathot V. The molecular theory of solutions. Amsterdam: North-Holland; 1957.
[3] Flory PJ, Orwoll RA, Vrij A. J Am Chem Soc 1964;86:3567.

[4] (a) Simha R, Somcynsky T. Macromolecules 1969;2:342.
(b) Somcynsky T, Simha R. J Appl Phys 1971;42:4545.
[5] Sanchez IC, Lacombe RH. J Phys Chem 1976;80:2353.
[6] Hartmann B, Haque MA. J Appl Polym Sci 1985;30:1553.
[7] Dee GT, Walsh DJ. Macromolecules 1988;21:811 [see also p. 815].
[8] Tait PG. (Rept Sci Results Voy HMS Challenger) Phys Chem 1888;2:1.
[9] Curro JG. J Macromol Sci, Rev Macromol Chem 1974;C11:321.
[10] Zoller P. In: Brandrup J, Immergut EH, editors. Polymer handbook. 3rd ed. New York: Wiley; 1989.
[11] Rodgers PA. J Appl Polym Sci 1993;50:1061.
[12] Rudolf B, Kressler J, Shimomami K, Ougizawa T, Inoue T. Acta Polym 1995;46:312.
[13] Ougizawa T, Dee GT, Walsh DJ. Polymer 1989;30:1675.
[14] Utracki LA, Simha R. Polym Int 2004;53:279.
[15] Utracki LA. J Polym Sci, Part B: Polym Phys 2004;42:2909.
[16] Utracki LA, Simha R. Macromol Chem Phys, Mol Theory Simul 2001;10:17.
[17] (a) Simha R, Jain RK, Jain SC. Polym Compos 1984;5:3.
(b) Papazoglou E, Simha R, Maurer FHJ. Rheol Acta 1989;28:302.
[18] (a) Simha R, Utracki LA, Garcia-Rejon A. Compos Interfaces 2001;8:345.
(b) Utracki LA, Simha R, Garcia-Rejon A. Macromolecules 2003;36:2114.
[19] Tanoue S, Utracki LA, Garcia-Rejon A, Tatibouët J, Cole KC, Kamal MR. Polym Eng Sci 2004;44:1046.
[20] Utracki LA, Simha R. Macromolecules 2004;37:10123.
[21] Utracki LA. J Rheol 1986;30:829.
[22] Utracki LA, Simha R. J Polym Sci, Part B: Polym Phys 2001;39:342.
[23] (a) Lennard-Jones JE. In: Fowler RH, editor. Statistical mechanics. Cambridge: University Press; 1929.
(b) Lennard-Jones JE. Proc Phys Soc 1931;43:461.
(c) Lennard-Jones JE, Devonshire AF. Proc Roy Soc 1937;163:53.
[24] Simha R. Macromolecules 1977;10:1025.
[25] Hirschfelder JO, Curtis CF, Bird RB. Molecular theory of gases and liquids. New York: Wiley; 1954.
[26] Utracki LA. Can J Chem Eng 1983;61:753.
[27] Utracki LA. Polym Eng Sci 1985;25:655.
[28] Zoller P, Walsh D. Standard pressure–volume–temperature data for polymers. Lancaster-Basel: Technomic; 1995.
[29] Quach A, Simha R. J Appl Phys 1971;42:4592.
[30] Hartmann B, Simha R, Berger AE. J Appl Polym Sci 1989;37:2603.
[31] Table I-A in Ref. [25].
[32] Schiessler RW, Dixon JA, Webb W. American Petroleum Institute Research Project 42, University Park: The Pennsylvania State University; 1940–1955.
[33] (a) Fox TG, Flory PJ. J Appl Phys 1950;21:581.
(b) Fox TG, Flory PJ. J Polym Sci 1954;14:315.
[34] Fox TG, Loshaek S. J Polym Sci 1955;15:371.
[35] (a) Nieuwenhuizen ThM. J Phys Condens Mater 2000;12:6543.
(b) Kanaya T, Kaji K. Adv Polym Sci 2001;154:87.
(c) Binder K, Baschnagel J, Paul W. Prog Polym Sci 2003;28:115.
[36] Hay G, Mackay ME, Hawker CJ. J Polym Sci, Part B: Polym Phys 2001;39:1766.
[37] Utracki LA. J Appl Polym Sci 2002;84:1101.
[38] Lewis DT. J Chem Soc 1938;1056.
[39] Meissner HP, Redding EM. Ind Eng Chem 1942;34:521.